WILEY Applied Organometallic Chemistry

Synthesis of a new schiff base oxovanadium complex with melamine and 2-hydroxynaphtaldehyde on modified magnetic nanoparticles as catalyst for allyl alcohols and olefins epoxidation

Faezeh Farzaneh [iD] | Zeinab Asgharpour

Alzahra University, Iran

Correspondence
Faezeh Farzaneh, Alzahra University, Iran.
Email: faezeh_farzaneh@yahoo.com; farzaneh@alzahra.ac.ir

A new magnetically recoverable nanocatalyst designated as $Fe_3O_4@SiO_2@PTMS@Mel-Naph-VOcomplex$ was synthesize by covalent binding of a Schiff base ligand derived from melamine and 2-hydroxy1naphtaldehyde on the surface of silica coated iron oxide magnetic nanoparticles followed by complexation with VO $(acac)_2$. Characterization of the prepared nanocatalyst was accomplished with FT-IR, XRD, SEM, HRTEM, VSM and atomic absorption techniques. It was found that the epoxidation of geraniol, *trans*-2-hexen-1-ol, 1-octen-3-ol, norbornene, and cyclooctene is highly selective, affording quantitative yields of the corresponding epoxides with *tert*-butyl hydroperoxide (TBHP) using $Fe_3O_4@SiO_2@Mel-Naph-VOcomplex$ as catalyst. High reaction yields, short reaction times, simple experimental and work up procedure, catalyst stability and excellent reusability even after five-cycles of usage in the case of geraniol are some advantages of this research.

KEYWORDS
epoxidation allylalcohols, melamine, modified magnetic nanoparticles, olefins, vanadium Schiff base complex

1 | INTRODUCTION

The enzymatic role and importance of vanadium compounds in biological catalytic systems such as bromoperoxidase and nitrogenase has created attention in the synthesis and catalytic activities of vanadium complexes.[1–4] Catalytic oxidation by metal complexes is one of the most widely studied reactions in organic chemistry since epoxides are important synthetic intermediates for a wide variety of products.[5–8] Oxovanadium complexes have been widely used as homogeneous and heterogeneous catalysts for reactions such as alkene epoxidations,[9] sulfoxidation,[10] alcohol oxidations,[11] oxidative couplings,[12] oxidative brominations,[13] oxidative Strecker reactions,[14] olefin polymerization[15] and carbon–carbon cleavages.[16]

In recent years, different types of vanadium coordination compounds with Schiff base ligands were synthesized and used as homogeneous and heterogeneous catalysts in the epoxidation reactions.[17–22] Moreover, to modify the stabilization and recycling ability of the homogeneous catalysis systems, they have been immobilized onto the solid supports. Various organic polymers[23] and inorganic materials such as silica, MCM-41, SBA-15, zeolites and magnetic nanoparticles[24–28] have been used as support in heterogeneous catalysis systems. Among them, Fe_3O_4 magnetic nanoparticles have attracted great interest because of low cost,

high surface area, low toxicity and easily separation by applying an external magnetic field.[29,30] In this regard, vanadium complex with N,N-bis(3-salicylidenamino propyl)amine (salpr),[31] Cu Schiff base complex with histidine and glutaraldehyde,[32] vanadium Schiff base complex with histidine and glutaraldehyde[26], vanadium Schiff base complex with 1,2-bis(2-formyl naphthoxy)ethane,[33] manganese Schiff base complex with azo Schiff base [(Z)-5-({2,4-dichloro-6-hydroxyphenyl}diazenyl)-2-hydroxybenzaldehyde,[34] *manganese* Schiff base complex with 2, 2-dimethylpropylenediamine and 5-bromo-2-hydroxybenzaldehyde,[35] molybdenum Schiff base complex with terephthaldehyde and thiosemicar bazide,[36] Cu^{2+} Schiff base complex with 3-aminopropyl (triethoxy) silane and 5-bromo-2-hydroxybenzalde hyde[37] immobilized on modified Fe_3O_4 nanoparticles have been used as catalyst for different organic transformation reactions. We are pleased to describe the synthesis of a new Schiff base oxovanadium complex with melamine and 2-hydroxynaphtaldehyde immobilized on the modified magnetic nanoparticles and using it as catalyst in the epoxidation of allyl alcohols and olefins.

2 | EXPRIMENTAL

2.1 | Materials and instrumentation

All materials were of commercial reagent grade and used without further purification. FT-IR spectra were recorded on a Bruker Tensor 27 FT-IR spectrometer using KBr pellets over the range of 4000–400 cm^{-1}. Scanning electron micrograph (SEM) images were taken by XL-30 Phillips (1992). High-resolution transmission electron microscopy (HRTEM) images were taken by FEI-Tecnai F20. Magnetic susceptibility measurements were carried out using a vibrating sample magnetometer (VSM) (BHV-55, Riken, Tehran, Iran) in the magnetic field range of −8000 to
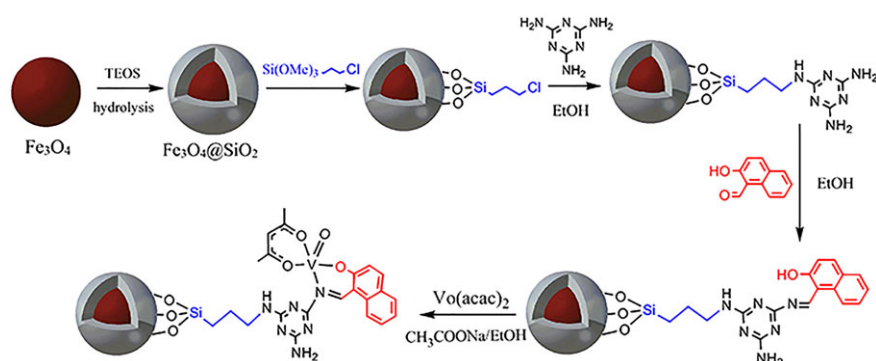

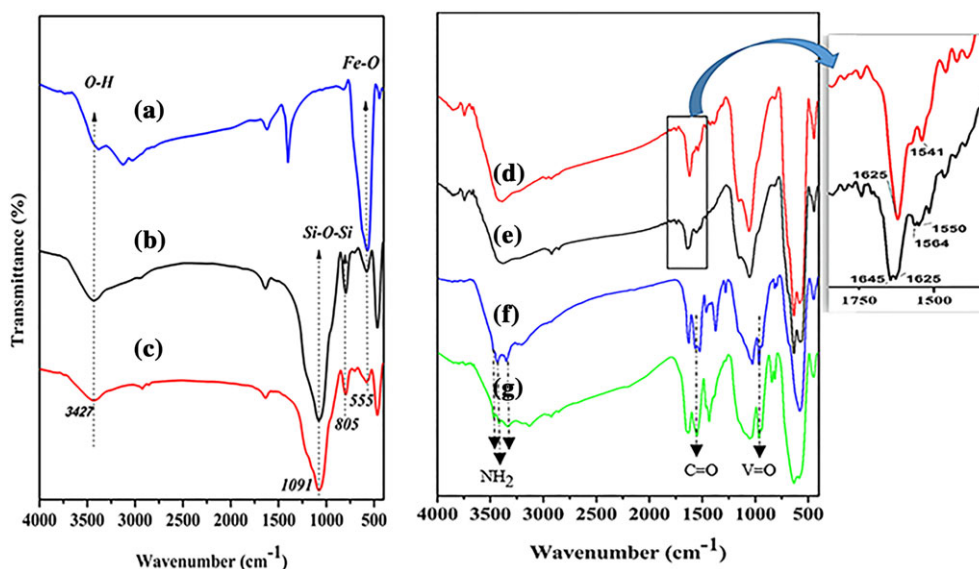
FIGURE 1 Preparation of Fe3O4@SiO2@PTMS@Mel-Naph-VOcomplex

FIGURE 2 FT-IR spectra of (a) Fe3O4, (b) Fe3O4@SiO2, (c) Fe3O4@SiO2@CPTMS, (d) Fe3O4@SiO2@PTMS@Melamine, (e) Fe3O4@SiO2@PTMS@Mela-Naph (f) Fe3O4@SiO2@ PTMS @Mel-NaphVO complex before using and (g) after using as catalyst

8000 Oe at room temperature. The X-ray powder diffraction (XRD) data were recorded on a Siefert XRD 3003 PTS diffractometer using Cu K_λ radiation (k = 1.5406 Å). Vanadium was determined by atomic absorption on a Chermo double beam instrument. Epoxidation products were analyzed by GC and GC-Mass using Agilent 6890 series with a FID detector, HP-5, 5% phenylmethylsiloxane capillary and Agilent 5973 network, mass selective detector, HP-5 MS 6989 network GC system, respectively.

2.2 | Preparation of modified magnetic nanoparticles

Fe_3O_4 as magnetic nanoparticle (MNPs), $Fe_3O_4@SiO_2$ silica coated magnetic nanoparticle (SCMNPs) and chlororopropyl modified SCMNPs ($Fe3O4@SiO_2@CPTMS$) designated as ClpSCMNPs were prepared as reported before (see also supplementary).[38,39]

2.3 | Preparation of schiff base of melamine and 2-hydroxynaphtaldehyde on the modified magnetic nanoparticles surface ($Fe_3O_4@SiO_2@PTMS@Mel-Naph$)

ClpSCMNPs (1.0 g) was suspended in EtOH (50 ml) and mixed with melamine (0.13 g, 1 mmol) and the mixture was heated at reflux for 24 hr. The resultant solid ($Fe_3O_4@SiO_2@PTMS@Melamine$) was separated magnetically and washed with EtOH and H_2O for several times and dried at room temperature. The obtained $Fe_3O_4@SiO_2@PTMS@Melamine$ nanoparticles (1.0 g) was then suspended in EtOH (50 ml) containing 2-hydroxy-1-naphtaldehyde (0.17 g, 1 mmol) and the mixture was heated at reflux for 24 hr. The obtained solid ($Fe_3O_4@SiO_2@Schiff$ base) was separated magnetically and washed with EtOH to remove the unreacted reagent and then dried in air.

2.4 | Preparation of $Fe_3O_4@SiO_2@PTMS@MeL-Naph-VOcomplex$ nanoparticles

$Fe_3O_4@SiO_2@Schiff$ base (1.0 g) was added to a solution of VO $(acac)_2$ (1 mmol in 50 ml EtOH) and the mixture was heated at reflux for 12 hr. The solid product was then separated magnetically, washed with EtOH and dried in air.

2.5 | Catalytic reactions

Typically, a desired amount of catalyst, substrate (10 mmol), solvent (5 ml) and TBHP (12 mmol) were mixed in the reaction flask. The suspension was then
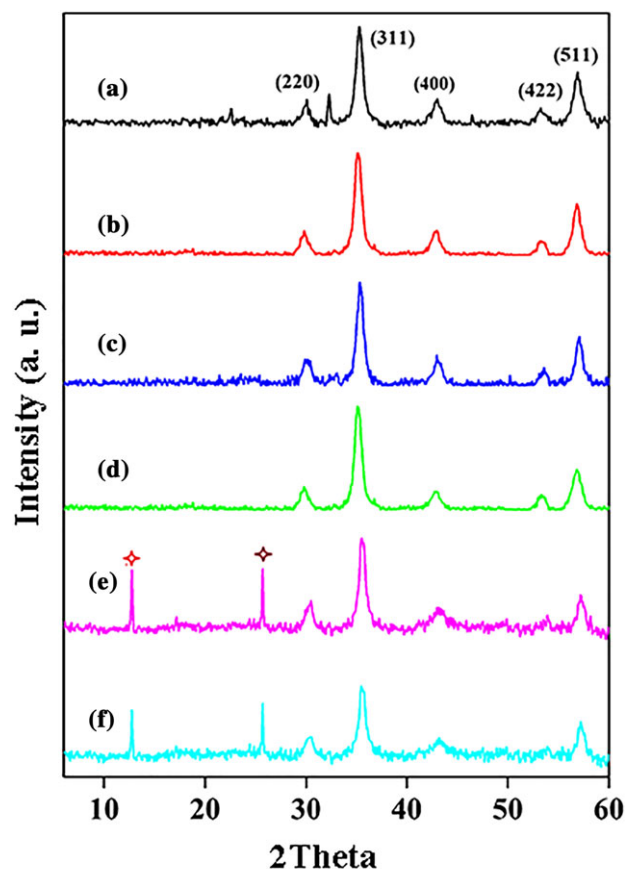

FIGURE 3 XRD pattern of (a) Fe3O4, (b) Fe3O4@SiO2, (c) Fe3O4@SiO2@CPTMS, (d) Fe3O4@SiO2@PTMS@ Mel-Naph (e) Fe3O4@SiO2@PTMS@Mel-Naph-VOcomplex before using and (f) after using as catalyst
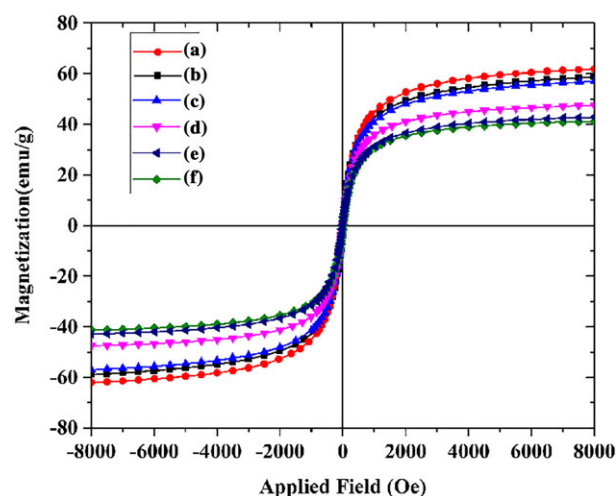
FIGURE 4 Magnetization curves of (a) Fe3O4, (b) Fe3O4@SiO2, (c) Fe3O4@SiO2@CPTMS, (d) Fe3O4@SiO2@PTMS@Mel-Naph (e) Fe3O4@SiO2@PTMS@Mel-Naph-VOcomplex before using and (f) after using as catalyst

heated at reflux for the desired time. After the separation of the catalyst using an external magnetic field, the solution was subjected to GC and GC–MS.

3 | RESULT AND DISCUSSION

3.1 | Synthesis of Fe$_3$O$_4$@SiO$_2$@PTMS @Mel-Naph-VOcomplex

Fe$_3$O$_4$ magnetic nanoparticles (MNPs) were prepared by precipitation of iron (II) and (III) ions in basic solution under nitrogen atmosphere. Subsequently, it was coated with silica to forming Fe$_3$O$_4$@SiO$_2$ core-shell particles followed by modification with (3-chloropropyl)trimetho xysilane to afford MNPs, designated as ClpSCMNPs (Fe$_3$O$_4$@SiO$_2$@CPTMS).[26,32] The next step involved grafting of melamine on the Fe$_3$O$_4$@SiO$_2$@CPTMS surface. Binding of 2-hydroxy-1-naphtaldehyde with Fe$_3$O$_4$@SiO$_2$@PTMS@Melamine to Schiff base followed by complexation with VO (acac)$_2$ finally afforded Fe$_3$O$_4$@SiO$_2$@PTMS@Mel-Naph-VOcomplex (Figure 1).

3.2 | Charactrization of Fe$_3$O$_4$@SiO$_2$ @PTMS@Mel-Naph-vocomplex

FT-IR spectra of the prepared Fe$_3$O$_4$, Fe$_3$O$_4$@SiO$_2$, Fe$_3$O$_4$@SiO$_2$@CPTMS Fe$_3$O$_4$@SiO$_2$@PTMS@Melamine, Fe$_3$O$_4$@SiO$_2$@PTMS@Mel-Naph (Schiff base), Fe$_3$O$_4$ @SiO$_2$@PTMS@Mel-Naph-VOcomplex before and after reaction, are shown in Figure 2a-g, respectively. Whereas the peak observed at 555 cm^{-1} is attributed to the Fe–O vibrations of Fe$_3$O$_4$ (MNPs) (Figure 2a), those centered at 1091 and 805 cm^{-1} assigned to the asymmetric and symmetric stretching vibrations of Si–O–Si confirm the successful coating of magnetite nanoparticles with silica (Figure 2b).[40] The two obvious bands appearing at 2870 and 2920 cm^{-1} due to the C-H stretching vibrations also confirm the functionalization of the modified Fe$_3$O$_4$@SiO$_2$ with ClPTMS, which was designated as Fe$_3$O$_4$@SiO$_2$@CPTMS (Figure 2c).[41] In the FT-IR

spectrum of Fe$_3$O$_4$@SiO$_2$@PTMS@Melamine, two new peaks appeared at 1625 and 1541 cm^{-1} are due to melamine C=N stretching and N-C-N bending vibrations (Figure 2d).[42] Based on these bands, successful grafting of melamine onto the Fe$_3$O$_4$@SiO$_2$@CPTMS nanoparticles surface is concluded. The formation of Schiff base ligand on the modified iron magnetic nanoparticles is further confirmed by observing a band at 1645 cm^{-1} due to the newly formed azomethine C=N and two others at 1564 and 1550 cm^{-1} for C-C stretching vibrations (Figure 2e). After complexation of VO (acac)$_2$ with Fe$_3$O$_4$@SiO$_2$@Schiff base, appearing NH$_2$ stretch peaks at 3469, 3419 and 3344 cm^{-1} and two peaks attributed to C=O and V=O stretching vibrations at 1568 and 961 cm^{-1} prove the formation of Fe$_3$O$_4$@SiO$_2$@PTMS@Mel-Naph (Figure 2f).[43–45]

The X-ray powder diffraction patterns of Fe$_3$O$_4$, Fe$_3$O$_4$@SiO$_2$, Fe$_3$O$_4$@SiO$_2$@CPTMS, Fe$_3$O$_4$@SiO$_2$@PT MS@Melamine, Fe$_3$O$_4$@SiO$_2$@PTMS@Mel-Naph (Fe$_3$O$_4$ @SiO$_2$@Schiff base), Fe$_3$O$_4$@SiO$_2$@PTMS@Mel-Naph-VO (acac) before and after reaction are shown in Figure 3a-f respectively. As shown in Figure 3a, it can
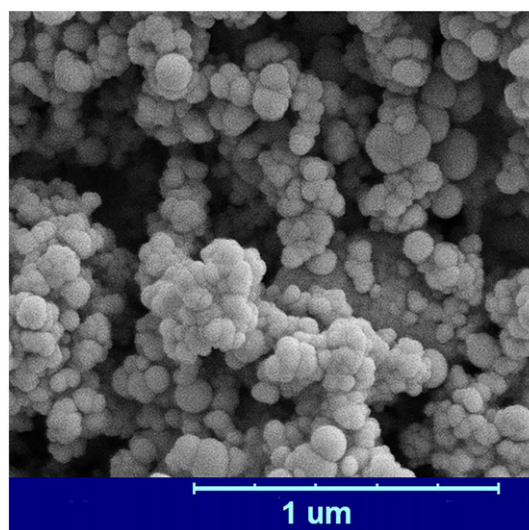

FIGURE 6 The SEM image of Fe3O4@SiO2@PTMS@Mel-Naph-VOcomplex
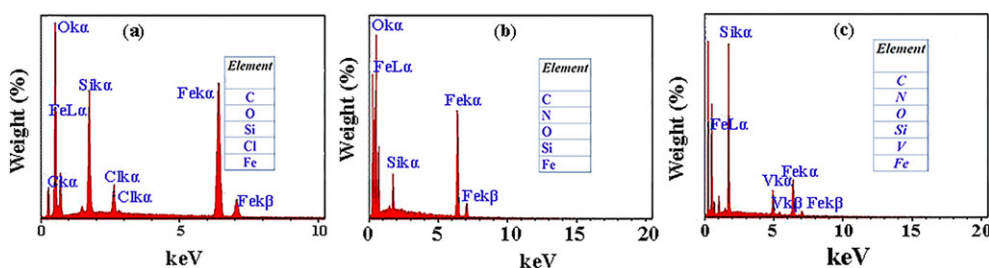
FIGURE 5 EDX spectra of (a) Fe3O4@SiO2@CPTMS, (b) Fe3O4@SiO2@PTMS@Mel-Naph, (c) Fe3O4@SiO2@Mel-Naph-VO complex
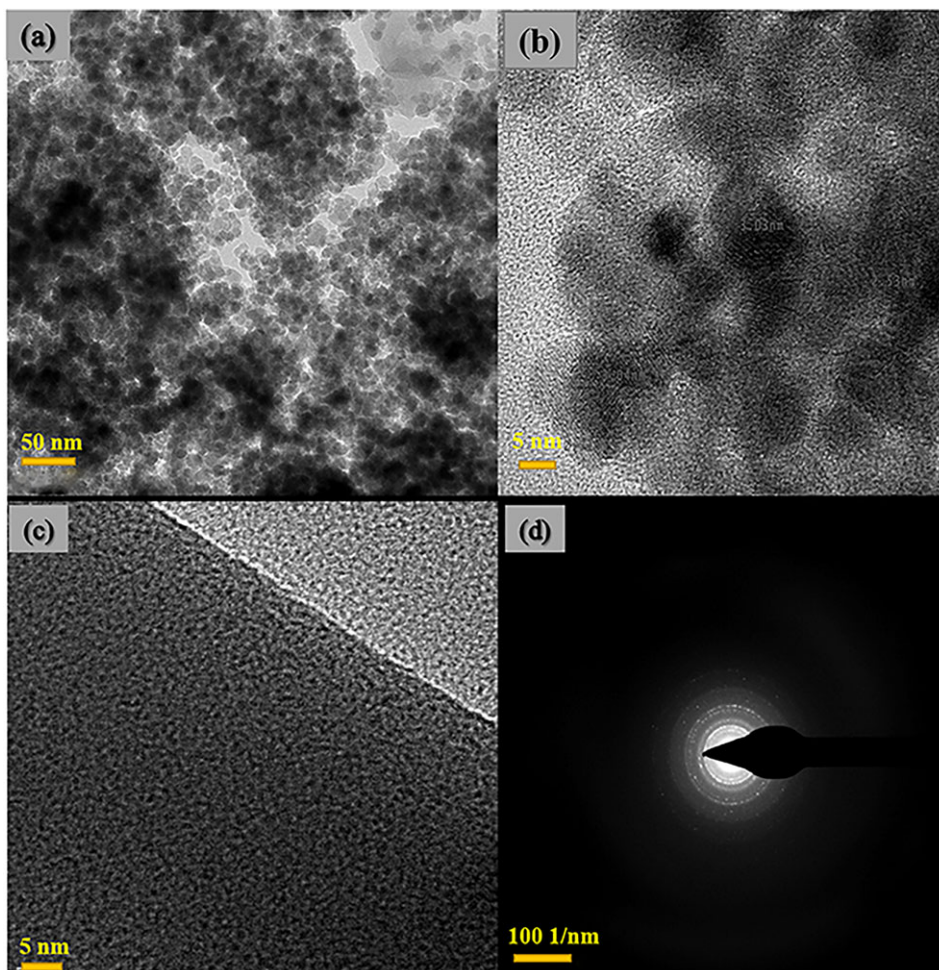
FIGURE 7 The HRTEM image of Fe3O4@SiO2@PTMS@Mel-Naph-VOcomplex(a, b) with two different magnification, (c) The dark and white tissue should be due to core and shell part of single nanoparticle (d) Selected area electron diffraction (SAED) of crystalline phase of nanoparticles

be seen that the Fe_3O_4 shows highly crystalline cubic spinel structure which agrees with the standard Fe_3O_4 (cubic phase) XRD pattern (JCPDSNo.19–0629).[46,47] The same set of characteristic peaks were also observed for $Fe_3O_4@SiO_2$, $Fe_3O_4@SiO_2@CPTMS$, $Fe_3O_4@SiO_2@PTMS@Melamine$ and $Fe_3O_4@SiO_2@PTMS @Mela-Naph$ (Schiff base). The obtained results indicate the stability of crystalline phase of Fe_3O_4 nanoparticles during the modification (Figure 3b-d). Observation of two new diffraction peaks at $2\theta = 12.7$ and $2\theta = 25.6$ confirms the formation of $Fe_3O_4@SiO_2@PTMS@Mel-Naph-VO$ complex (Figure 3e).

The magnetic properties of Fe_3O_4, $Fe_3O_4@SiO_2$, $Fe_3O_4@SiO_2@CPTMS$, $Fe_3O_4@SiO_2@PTMS@Mela-Naph$, $Fe_3O_4@SiO_2@PTMS@Mel-Naph-VOcomplex$ before and after reaction were examined by vibrating sampling magnetometry (VSM) at room temperature (Figure 4a-f). The magnetization curve of Fe_3O_4 exhibits superparamagnetic property with saturation magnetization of about 61 emu/g (Figure 4a). Superparamagnetic behavior of the

silica coated Fe_3O_4 magnetite nanoparticles was determined to be 58.8 emu/g (Figure 4b). The superparamagnetic behavior of $Fe_3O_4@SiO_2@CPTMS$ and $Fe_3O_4@SiO_2@CPTMS@$ Mel-Naph (Schiff base) were also found 57 emu/g and 47.5 emu/g respectively (Figure 4c,d). After

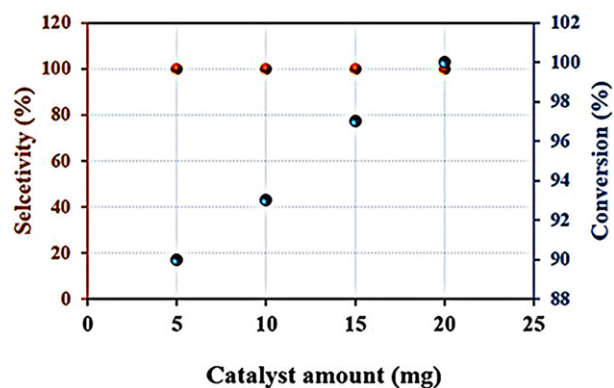**FIGURE 8** Conversion and Selectivity of geraniol with different amounts of Fe3O4@SiO2@PTMS@-MelNaph-VOcomplex

formation of Fe$_3$O$_4$@SiO$_2$@PTMS@Mel-Naph-VO (acac), superparamagnetic behavior was found to be 43 emu/g (Figure 4e).

The EDX for Fe$_3$O$_4$@SiO$_2$@CPTMS, Fe$_3$O$_4$@SiO$_2$@PTMS@Mel-Naph and Fe$_3$O$_4$@SiO$_2$@PTMS@Mel-Naph-VOcomplex are shown in Figure 5a-c, respectively. Based on the obtained results, characteristic peaks containing C, O, Si, Cl and Fe are indicative of the presence of these atoms in for Fe$_3$O$_4$@SiO$_2$@CPTMS nanoparticles (Figure 5a). After formation of Schiff base on the nanomagnet surface, no peak due to the presence of chlorine atom is observed but the presence of nitrogen is considerable (Figure 5b). Based on the obtained results with EDX, the Cl has been exchanged with melamine hydrogen. The presence of vanadium determined in the Fe$_3$O$_4$@SiO$_2$@Mel-Naph-VO (acac) EDX also confirms the formation of the proposed structure (Figure 5c).

The SEM image of Fe$_3$O$_4$@SiO$_2$@PTMS@Mel-Naph-VOcomplex indicates the morphology of nanoparticles (Figure 6). HRTEM images of Fe$_3$O$_4$@SiO$_2$@PTMS @Mel-Naph-VOcomplex with two magnification are shown in Figure 7 a-b, respectively The obtained results indicate the formation of core and shell of nanoparticles with particle size of about 10–15 nm. The dark and white tissue seen in Figure 7c should be due to core and shell part of single nanoparticle. Selected area electron diffraction (SAED) of crystalline phase is shown in Figure 7d. The ring patterns are due to the crystalline planes of the prepared nanoparticles.

3.3 | Catalytic activity of Fe$_3$O$_4$ @SiO$_2$@-Mel-Naph-VOcomplex

The catalytic activity of Fe$_3$O$_4$@SiO$_2$@-Mel-Naph-VOcomplex was studied in the epoxidation of some allyl alcohols and alkenes in acetonitrile. TBHP was used as oxidant due to its high oxidation selectivity behavior. Geraniol served for our early exploration of allyl alcohol epoxidations in order to find the optimum reaction conditions. Various parameters such as the effect of catalyst amount, reaction time and solvent were evaluated. To optimize the catalyst amount, reaction was carried out using 5, 10, 15 and 20 mg of catalyst in acetonitrile while
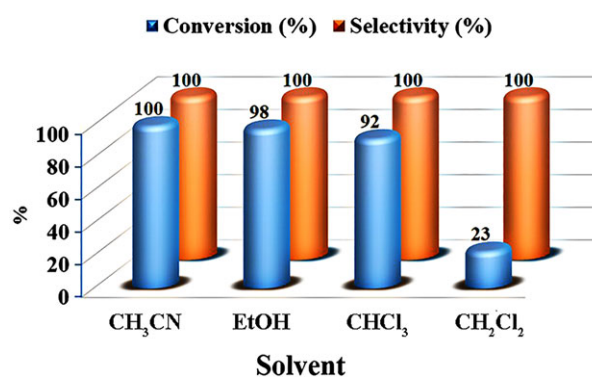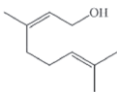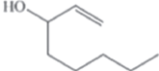

FIGURE 9 The effect of solvent on the conversion and selectivity of geraniol using Fe3O4@SiO2@PTMS@Mel-Naph-VOcomplex as catalyst

TABLE 1 Results obtained for the epoxidation of allyl alcohols

Entry	Substrate	Time (h)	Conversion[a] (%)	Epoxide (%)	TON[b]	TOF[c] (h^{-1})
1	Geraniol	0.5	85	100		
		1.0	93	100		
		1.5	97	100		
		2.0	100	100	833	417
2	trans-2-Hexene-1-ol	0.5	74	100		
		1.0	81	100		
		1.5	87	100		
		2.0	93	100		
		3.0	100	100	833	278
3	1-Octene-3-ol	1.0	67	100		
		1.5	73	100		
		2.0	81	100		
		3.0	91	100		
		4.0	96	100		
		5.0	100	100	833	167

[a]Reaction condition: catalyst (20 mg), allyl alchohol (10 mmol), TBHP (12 mmol), in CH$_3$CN, heated to reflux.

[b]TON is the mmol of epoxide to the mmol of vanadium present in the catalyst.

[c]TOF: turnover frequency which is calculated by the expression of [epoxide]/[catalyst]time.

FIGURE 10 Result of epoxidation of allyl alcohols in presence of Fe3O4@SiO2@PTMS@-Mel-NaphVOcomplex. Reaction condition: catalyst (20 mg), allyl alchohol (10 mmol), TBHP (12 mmol), solvent CH3CN

heating at reflux within 2 hr. As seen in Figure 8, increasing the amount of catalyst from 5 to 20 mg increases the conversion from 90 to 100% with 100% selectivity toward the formation of geraniol epoxide. Thereafter, all epoxidation reactions were carried out using 20 mg of catalyst.
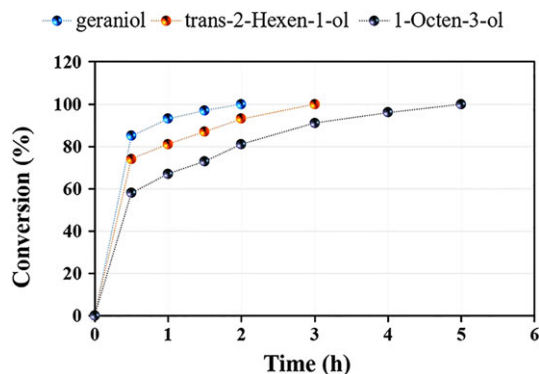
The effect of time on the geraniol conversion was investigated using 20 mg of catalyst. Increasing the reaction time from 0.5 to 2 hr was found to increase the geraniol conversion from 85 to 100% with 100% selectivity (entry 1, Table 1).

Finally, a variety of solvents such as CH_3CN, C_2H_5OH, $CHCl_3$ and CH_2Cl_2 were tested for the epoxidation of geraniol. As seen in Figure 9, the catalytic activity trend was found to be:

CH_3CN~ C_2H_5OH > $CHCl_3$ > CH_2Cl_2. Therefore, other allyl alcohols epoxidation reactions were carried out in CH_3CN. Based on the obtained results, the highest conversion of geraniol epoxidation reaction occurs in CH_3CN and ethanol. The higher boiling points of the solvents seems to be responsible for solvent trend simply because more geraniol conversion occurs at higher temperature.

In the next step, the epoxidation of *trans*-2- hexen-1-ol and 1-octen-3-ol were investigated in CH_3CN using 20 mg of catalyst within 0.5 to 5 hr. As seen in Figure 10, *trans*-2- hexen-1-ol and 1-octen-3-ol were converted to the corresponding epoxides with 100% conversions and selectivities within 3 and 5 hr, respectively (entries 2–3, Table 1).

Finally, H_2O_2 and O_2 were used as oxidant in the epoxidation of geraniol under optimal conditions. It was found that whereas reaction proceeds about 10% using H_2O_2, no conversion occurred in the presence of O_2.

The decrease in conversion rates from geraniol to *trans*-2-hexen-1-ol and 1-octen-3-ol may be realized on the basis of the suggested mechanism shown in Scheme 1. After the formation of intermediates **I** and **II** upon the initial coordination of TBHP and allyl alcohol to the catalyst vanadium
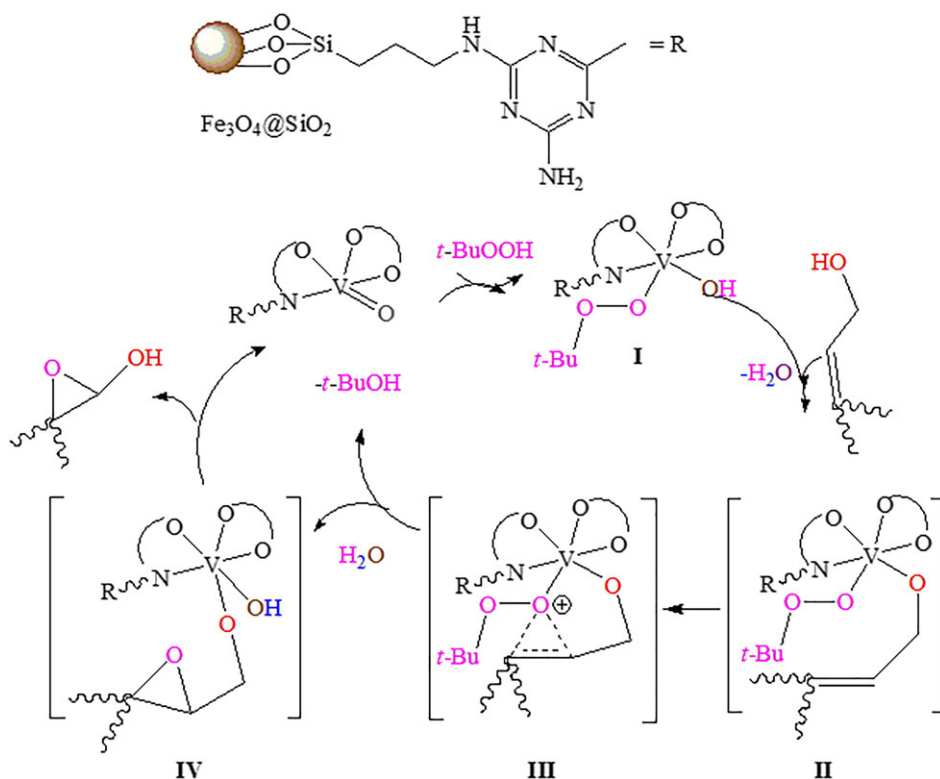
SCHEME 1 Suggested mechanism for the epoxidation of allyl alcohols

core, the allyl alcohol is subsequently oxygenated by nucleophilic attack of the double bond to the electrophilic oxygen atom of the coordinated TBHP peroxide with generation of **III**. In the next step, addition of water to vanadium in **III** affords **IV**. Finally, concomitant elimination of *tert*-butanol and epoxide regenerates the catalyst (Scheme 1). Since the formation rate of **III** in the nucleophilic attack of double bond to the oxygen electrophile depends on the number of alkyl substitutions present on the double bonds,[27] it can be concluded that the geraniol which contains a trisubstituted double bonds exhibit the highest epoxidation rate. On the other hand, *trans*-2-hexen-1-ol and 1-octen-3-ol containing disubstituted and monosubstituted double bonds would undergo epoxidation reactions in lower rates, respectively.

To further support the operation of a concerted mechanism, reaction was carried out in the presence of diphenylamine as radical scavenger.[48] Observation of no conversion inhibition indicated that reaction does not proceed through a radical mechanism.
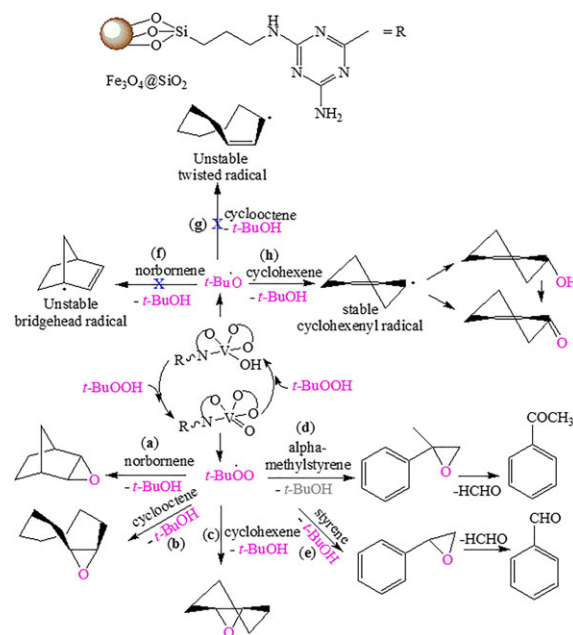
SCHEME 2 Suggested mechanism for the epoxidation of alkenes

TABLE 2 result of epoxidation of olefines in different times

Entry	Substrate	Time (h)	Conversion[a] (%)	Selectivity(%)	TON[b]	TOF[c] (h^{-1})
1	Norbornene	2	37	100		
		4	50	100		
		6	75	100		
		8	92	100	833	104
2	Cyclooctene	2	32	100		
		4	45	100		
		6	60	100		
		8	80	100	833	104
3	Cyclohexene	2	8	60		
		4	12	64		
		6	16	65		
		8	45[d]	70	583	73
4	α-methylstyrene	2	36	60		
		4	50	65		
		6	64	67		
		8	75[e]	74	6	77
5	Styrene	2	16	48		
		4	23	50		
		6	31	56		
		8	56[f]	58	483	60

[a]Reaction condition: catalyst (20 mg), alkene (10 mmol), TBHP (12 mmol), refluxing CH3CN.

[b]TON is the mmol of epoxide to the mmol molybdenum present in catalyst.

[c]TOF: turnover frequency which is calculated by the expression [epoxide]/[catalyst]×time (h^{-1}).

[d]The side product is 2-cyclohexene-1-one.

[e]The side product is acetophenone.

[f]The side product is benzaldyde.

In the next step, alkenes such as norbornene, cyclooctene, cyclohexene, α-methyl styrene and styrene were oxidized with TBHP in acetonitrile using Fe_3O_4 @SiO$_2$@Mel-Naph-VOcomplex as catalyst (Table 2). As seen in Table 2, whereas norbornene and cyclooctene exclusively give the corresponding epoxides (entry 1–2, Table 2), cyclohexene, α-methyl styrene and styrene epoxidations afford other side products in addition to epoxides (entries 3–5, Table 2). Observation of two oxidation paths in cyclohexene clearly specifies that not only reaction of alkene double bounds with t-BuOO radical generate the corresponding epoxides (Scheme 2a-e), but also if an allylic H abstraction occur, it is followed by the formation of the corresponding allylic radicals. Whereas norbornene results in the formation of extremely unstable bridgehead radical (Scheme 2f), cyclooctene generates an unstable intermediate since the double bond is in one plane and all other carbons are in another plane (Schemes 2g).[49] On the other hand and in oppose to cyclooctenyl radical, cyclohexene partly undergoes allylic-site oxidation since the C–H bond is close to parallel to the C=C orbital in its half-chair conformation (Scheme 2h).[50] Therefore, the formation of 2-cyclohexene-1-one identified as the side products is rationalized (footnote d, Table 2). Finally, the generation of acetophenone (Scheme 2d) and benzaldehyde (Scheme 2e) respectively in the epoxidation of methylstyrene (footnote e, Table 2) and styrene (footnote f, Table 2) is not surprising since the partial hydrolysis of the α-methyl styrene and styrene epoxides in the aqueous solution of the used TBHP as oxidant has been reported previously.[51]

The reusability of the catalyst for epoxidation reaction of geraniol with TBHP was carried out under the optimized reaction conditions. In this regard, the catalyst was separated by external magnet from reaction mixture after completion of the first run. It was washed with acetonitrile and dried before using in the next runs. Based on the collected data, it was concluded that the catalyst can be reused for five consecutive cycles with slight decrease in activity from 99 to 96% (Figure 11).

On the other hand, since no catalytic activity was observed upon the subjection of the filtrate to the new epoxidation reaction in the absence of the catalyst, the heterogeneity of catalyst function was concluded.

The vanadium content of the catalyst before and after use in reaction was determined as 3.07%. and 3.03%, respectively. It was concluded that no significant catalyst
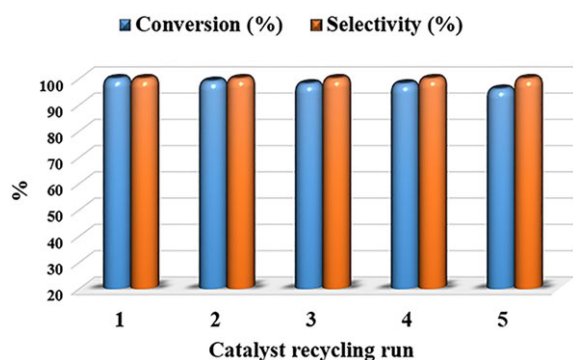

FIGURE 11 The effect of recycling on epoxidation of geraniol

TABLE 3 Catalytic activities toward the epoxidation of geraniol of some previously reported heterogeneous catalysts

Entry	Catalyst	Conversion (%)	Selectivity (%)	TON	TOF(h^{-1})	Ref.
1	Fe$_3$O$_4$ @ SiO$_2$ @ PTMS @ Mel-Naph-VO	100	100	834	417	This work
2	Osalpr @ SCMNPs	100	100	746	187	[31]
3	8-quinolinol oxovanadium (IV) complex @ graphene oxide	83.7	80	199	25	[52]
4	Fe$_3$O$_4$@SiO$_2$@APTMS@[VO$_2$(bpca)]	100	100	155	155	[27]
5	CMK-3 @ [VO (acac)$_2$]	100	97	100	91	[53]
6	CMK3 @ APTES @ [VO (acac)$_2$]with amine	98	98	74	68	[53]
7	VO (Sa l-His) @ Al-MCM-41	100	99	4040	505	[54]
8	VO @ AlMCM41	27	77	3375	422	[54]
9	Fe$_3$O$_4$ @ SiO$_2$ @ APTMS@VMIL-101	96	97	1185	184	[55]
10	[VO (acac)$_2$] APTES @ SiO$_2$	100	99	34	17	[56]
11	Fe$_2$O$_3$ @ SiO$_2$–NH2–Vo (acac)$_2$	100	96	60	2	[57]
12	[VO (acac)$_2$] @ APTES @ laponite	100	97	96	2	[58]
13	[VO (acac)$_2$] @ APTES@K10	100	98	96	2	[58]
14	[VO (acac)$_2$] @ hexagonal mesoporous silica	98	98	96	2	[59]
15	[VO (acac)$_2$]APTES @ PCH	42	81	-	-	[60]
16	[VO (acac)$_2$]APTES @ SBA-15	34	88	-	-	[60]

desorption occurs during the course of reaction. More-over, the similarity observed in the XRD pattern and FTIR spectrum of the catalyst before and after using in geraniol epoxidation further revealed the stability and heterogeneity character of the nanocatalyst.

Finally, comparison of the epoxidation results of geraniol catalyzed by $Fe_3O_4@SiO_2@CPTMS@$-Mel-Naph-VOcomplex in this work with some previously reported heterogeneous catalysts provided in Table 3 reveals that conversion, selectivity, TON and TOF of our catalysis system is considerable.[27,31,52–60]

4 | CONCLUSION

In conclusion, the synthesis of a new magnetically recoverable nanocatalyst with modification of Fe_3O_4 magnetic nanoparticles by covalent binding of a Schiff base ligand, derived from melamine and 2-hydroxy1naphtaldehyde on the surface of magnetic nanoparticles followed by complexation with VO $(acac)_2$ was successfully carried out. After characterization, it was found that several allyl alcohols and alkenes can be selectively epoxidized in the presence of the prepared magnetically nanocatalyst. The stability, heterogeneity and excellent reusability of the catalyst even after five-cycles of usage in the case of geraniol epoxidation is promising.

ORCID

Faezeh Farzaneh 🄳 https://orcid.org/0000-0001-5651-8018

REFERENCES

[1] C. Leblanc, H. Vilter, J.-B. Fournier, L. Delage, P. Potin, E. Rebuffet, M. Czjzek, *Coord. Chem. Rev.* **2015**, *301*, 13.

[2] D. Wischang, M. Radlow, H. Schulz, H. Vilter, L. Viehweger, M. O. Altmeyer, F. Gaillard, *Bioorg. Chem.* **2012**, *44*, 25.

[3] J. C. Pessoa, E. Garribba, M. F. A. Santos, T. Santos-Silva, *Coord. Chem. Rev.* **2015**, *301*, 49.

[4] R. R. Eady, *Coord. Chem. Rev.* **2003**, *237*, 23.

[5] T. Punniyamurthy, S. Velusamy, J. Iqbal, *Chem. Rev.* **2005**, *105*, 2329.

[6] V. Conte, A. Coletti, B. Floris, G. Licini, C. Zonta, *Coord. Chem. Rev.* **2011**, *255*, 2165.

[7] M. Kirihara, *Coord. Chem. Rev.* **2011**, *255*, 2281.

[8] A. G. Ligtenbarg, R. Hage, B. L. Feringa, *Coord. Chem. Rev.* **2003**, *237*, 89.

[9] M. Mirzaee, B. Bahramian, M. Mirebrahimi, *Chin. J. Catal.* **2016**, *37*, 1263.

[10] N. Noori, M. Nikoorazm, A. Ghorbani-Choghamarani, *Micropor. Mesopor. Mater.* **2016**, *234*, 166.

[11] D. Kobayashi, S. Kodama, Y. Ishii, *Tetrahedron Lett.* **2017**, *5*, 3306.

[12] N. Noshiranzadeh, R. Bikas, M. Emami, M. Siczek, T. Lis, *Polyhedron* **2016**, *111*, 167.

[13] P. Pongpipatt, S. Saroachsoontornkul, W. Chavasiri, *Cat. Com.* **2018**, *109*, 10.

[14] C. Zhu, J. B. Xia, C. Chen, *Tetrahedron Lett.* **2014**, *55*, 232.

[15] J. Q. Wu, Y. S. Li, *Coord. Chem. Rev.* **2011**, *255*, 2303.

[16] E. Amadio, R. Di Lorenzo, C. Zonta, G. Licini, *Coord. Chem. Rev.* **2015**, *301*, 147.

[17] M. Sedighipoor, A. H. Kianfar, W. A. K. Mahmood, M. H. Azarian, *Inorg. Chim. Acta* **2017**, *457*, 116.

[18] V. Tahmasebi, G. Grivani, G. Bruno, *J. Mol. Struct.* **2016**, *1123*, 367.

[19] G. Grivani, A. Ghavami, V. Eigner, M. Dušek, A. D. Khalaji, *Chin.Chem. Lett.* **2015**, *26*, 779.

[20] Z. Abbasi, M. Behzad, A. Ghaffari, H. A. Rudbari, G. Bruno, *Inorg. Chim. Acta* **2014**, *414*, 78.

[21] S. Dorbes, C. Pereira, M. Andrade, D. Barros, A. M. Pereira, S. L. H. Rebelo, C. Freire, *Micropor. Mesopor. Mater.* **2012**, *160*, 67.

[22] J. Pisk, J. C. Daran, R. Poli, D. Agustin, *J. Mol. Catal. A: Chem.* **2015**, *403*, 52.

[23] M. R. Maurya, A. Arya, P. Adão, J. C. Pessoa, *Appl. Catal. Gen.* **2008**, *351*, 239.

[24] M. R. Maurya, A. Kumar, J. C. Pessoa, *Coord. Chem.Rev.* **2315**, *2011*, 255.

[25] C. Pereira, A. R. Silva, A. P. Carvalho, J. Pires, C. Freire, *J. Mol. Catal. A: Chem.* **2008**, *283*, 5.

[26] F. Farzaneh, Y. Sadeghi, M. Maghami, Z. Asgharpour, *J. Cluster Sci.* **2016**, *27*, 1701.

[27] Z. Azarkamanzad, F. Farzaneh, M. Maghami, J. Simpson, M. Azarkish, *Appl. Organomet. Chem.* **2018**, *32*, 4168.

[28] Z. Asgharpour, F. Farzaneh, A. Abbasi, *RSC Adv.* **2016**, *6*, 95729.

[29] A. H. Lu, W. Schmidt, N. Matoussevitch, H. Bönnemann, B. Spliethoff, B. Tesche, F. Schüth, *Angew. Chem.* **2004**, *116*, 4403.

[30] W. Yang, L. Wei, F. Yi, M. Cai, *Cat. Sci. Technol.* **2016**, *6*, 4554.

[31] L. Hamidipour, F. Farzaneh, *C. R. Chim.* **2014**, *17*, 927.

[32] F. Farzaneh, E. Rashtizadeh, *JICS* **2016**, *13*, 1145.

[33] H. Veisi, A. Rashtiani, A. Rostami, M. Shirinbayan, S. Hemmat, *Polyhedron* **2018**, *157*, 358. https://doi.org/10.1016/j.poly.2018.09.034

[34] F. Karami Olia, S. Sayyahi, N. Taheri, *C. R. Chim.* **2017**, *20*, 370.

[35] S. Rayati, E. Khodaei, M. Jafarian, A. Wojtczak, *Polyhedron* **2017**, *133*, 327.

[36] M. Mohammadikish, M. Masteri-Farahani, S. Mahdavi, *J. Magn. Magn. Mater.* **2014**, *354*, 317.

[37] A. Ghorbani-Choghamarani, B. Ghasemi, Z. Safari, G. Azadi, *Cat. Com.* **2015**, *60*, 70.

[38] X. Liu, Z. Ma, J. Xing, H. Liu, *J. Magn. Magn. Mater.* **2004**, *270*, 1.

[39] M. Masteri-Farahani, N. Tayyebi, *J. Mol. Catal. A: Chem.* **2011**, *348*, 83.

[40] J. Wang, S. Zheng, Y. Shao, J. Liu, Z. Xu, D. Zhu, *J. Colloid Interface Sci.* **2010**, *349*, 293.

[41] M. Masteri-Farahani, F. Farzaneh, M. Ghandi, *J. Mol. Catal. A: Chem.* **2006**, *243*, 170.

[42] N. A. Yusof, S. K. A. Rahman, M. Z. Hussein, N. A. Ibrahim, *Polymer* **2013**, *5*, 1215.

[43] S. Jawaid, F. N. Talpur, H. I. Afridi, S. M. Nizamani, A. A. Khaskheli, S. Naz, *Anal. Methods* **2014**, *6*, 5269.

[44] M. Esmaeilpour, J. Javidi, F. N. Dodeji, M. M. Abarghoui, *J. Mol. Catal. A: Chem.* **2014**, *393*, 18.

[45] R. Ando, S. Mori, M. Hayashi, T. Yagyu, M. Maeda, *Inorg. Chim. Acta* **2004**, *357*, 1177.

[46] F. Zhang, Z. Zhu, Z. Dong, Z. Cui, H. Wang, W. Hu, R. Li, *Microchem. J.* **2011**, *98*, 328.

[47] S.-K. Li, F.-Z. Huang, Y. Wang, Y.-H. Shen, L.-G. Qiu, A.-J. Xie, S.-J. Xu, *J. Mater. Chem. A* **2011**, *21*, 7459.

[48] L. M. Slaughter, J. P. Collman, T. A. Eberspacher, J. I. Brauman, *Inorg. Chem.* **2004**, *43*, 5198.

[49] J. March, *Advanced Organic Chemistry*, 3rd ed., Wiley, New York **1985**.

[50] F. A. Carey, R. J. Sundberg, Advanced organic chemistry, in *Part A: Structure and Mechanisms*, Fifth ed., Springer Science & Business Media, Plenum Press, New York 2007.

[51] V. Hulea, E. Dumitriu, *Appl. Cata. A: Gen.* **2004**, *277*, 99.

[52] Z. Li, S. Wu, D. Zheng, H. Liu, H. Ju, H. Su, J. Sun, X. Wang, Q. Huo, J. Guan, *Appl. Catal. A.* **2014**, *470*, 104.

[53] S. Dorbes, C. Pereira, M. Andrade, D. Barros, A. M. Pereira, S. Dorbes, C. Pereira, M. Andrade, D. Barros, A. M. Pereira, S. L. H. Rebelo, J. P. Araújo, J. Pires, A. P. Carvalho, C. Freire, *Micropor. Mesopor. Mat.* **2012**, *160*, 67.

[54] E. Zamanifar, F. Farzaneh, *Reac. Kinet. Mech. Cat.* **2011**, *104*, 197.

[55] F. Farzaneh, Y. Sadeghi, *J. Mol. Catal. A: Chem.* **2015**, *398*, 275.

[56] C. Pereira, J. F. Silva, A. M. Pereira, J. P. Araujo, G. Blanco, J. M. Pintado, C. Freire, *Cat. Sci. Technol.* **2011**, *1*, 784.

[57] C. Pereira, A. M. Pereira, P. Quaresma, P. B. Tavares, E. Pereira, J. P. Araújo, C. Freire, *Dalton Trans.* **2010**, *39*, 2842.

[58] J. C. Anderson, N. M. Smith, M. Robertson, M. S. Scott, *Tetrahedron Lett.* **2009**, *50*, 5344.

[59] B. Jarrais, C. Pereira, A. R. Silva, A. P. Carvalho, J. Pires, C. Freire, *Polyhedron* **2009**, *28*, 994.

[60] C. Pereira, K. Biernacki, S. L. Rebelo, A. L. Magalhães, A. P. Carvalho, J. Pires, C. Freire, *J. Mol. Catal. A: Chem.* **2009**, *312*, 53.

SUPPORTING INFORMATION

Additional supporting information may be found online in the Supporting Information section at the end of the article.